J. Chem. Sci. (2018) 130:40
https://doi.org/10.1007/s12039-018-1447-y

REGULAR ARTICLE

Oxidative Dehydrogenation (ODH) of Ethylbenzene with CO_2 and N_2O over Heteropolycompounds

SALEM CHEKNOUN*, SADIA MANSOURI, OUARDA BENLOUNES and SMAIN HOCINE
Laboratoire de Chimie Appliquée et de Génie Chimique, Université M. Mammeri de Tizi-Ouzou, BP 17, R.P. 1500 Tizi-Ouzou, Algeria
E-mail: cheknounsalem@yahoo.fr

MS received 27 November 2017; revised 24 February 2018; accepted 3 March 2018; published online 27 March 2018

Abstract. Heteropolyacids of Keggin structure, $H_3PMo_{12}O_{40}$, $H_3PMo_{11}WO_{40}$ and the salts $K_3PMo_{11}WO_{40}$ and $K_{2.5}Fe_{0.08}H_{0.26}PMo_{11}WO_{40}$ were characterized by X-ray diffraction (XRD), UV-Vis spectroscopy, Fourier transform infrared (FTIR), low-temperature nitrogen adsorption and ^{31}P MAS NMR spectroscopy. The acid-base properties were evaluated using the isopropanol decomposition. They were tested in oxidative dehydrogenation (ODH) of ethylbenzene in the temperature range 300–400 °C at atmospheric pressure with the mild oxidants carbon dioxide and nitrous oxide, the major actors in the greenhouse effect. The results show that the best compromise between conversion and selectivity is obtained for the mixed K/Fe salt of $PMo_{11}WO_{40}$ at a relatively low temperature, namely 350°C.

Keywords. Ethylbenzene; oxidative dehydrogenation; CO_2; N_2O; heteropolycompounds.

1. Introduction

Heteropolyanions (HPAs) are receiving increasing attention from both fundamental and industrial point of view because of their excellent acidic, redox and thermal stabilities and special catalytic properties. The beneficial effect of the incorporation of a transition metal cation on the oxidation properties of heteropolyoxometalates has already been reported in the literature.[1,2] Iron was found to be the most efficient element for propane and isobutene selective oxidation to acrylic or isobutyric acids, respectively.[1–6] Heteropolyoxometalates have been already tested as catalysts for oxidative dehydrogenation (ODH) and selective oxidation of alkanes and arylalkanes.[7–10]

Ethylbenzene is one of the most important arylalkanes, being a starting species in the chemical industry.[11] It has long been known that ethylbenzene can be oxidized, very selectively, to styrene over Fe_2O_3-K_2O catalysts with addition of one or more promoters, such as Cr_2O_3, MgO, MoO_3.[12,13] Dioxygen was first proposed to be the oxidizing agent. However, it appeared that the use of O_2 (strong oxidant) leads to complete oxidation of ethylbenzene to COx.

As an alternative to the strong oxidant O_2, carbon dioxide and nitrous oxide, the main contributors to the greenhouse effect, were proposed as non-traditional mild oxidants for catalytic oxidation of light alkanes.[14–17] In the present paper, we report on the catalytic activity of various HPAs on the ODH of ethylbenzene with CO_2 and N_2O as the oxidant.

2. Experimental

2.1 *Preparation of catalysts*

All the chemicals were purchased from Sigma-Aldrich (St. Louis, MO, USA) and used without further purification. The heteropolyacid $H_3PMo_{12}O_{40}$.aq (noted as $HPMo_{12}$) was prepared in two steps according to the literature.[18] The first is the preparation of the disodium salt $Na_2HPMo_{12}O_{40}.16H_2O$ and the second stage consists of isolating the heteropolyacid $H_3PMo_{12}O_{40}$ by extraction with diethyl-ether (Et_2O).

Step 1: 290 g (1.2 mol) of Na_2MoO_4, $2H_2O$ (99% purity) was dissolved in 420 mL distilled water. Then 6.8 mL of 85% H_3PO_4 (0.1 mol) and 284 mL of 70% $HClO_4$ (3.3 mol) were added successively. After the mixture was cooled to room temperature, the disodium salt $Na_2HPMo_{12}O_{40}$ was precipitated and filtered.

*For correspondence

Electronic supplementary material: The online version of this article (https://doi.org/10.1007/s12039-018-1447-y) contains supplementary material, which is available to authorized users.

Step 2: $H_3PMo_{12}O_{40} \cdot 14H_2O$ was obtained from an aqueous solution of $Na_2HPMo_{12}O_{40} \cdot 16H_2O$ (250 g/200 mL), acidified by 50 mL of 12 M HCl (37%) and extracted by 400 mL of Et_2O (99.5% purity). The heavy layer (300 mL), added with half its volume of water gave yellow crystals after desiccation (200 g).

$H_3PMo_{11}WO_{40}$ (noted as $HPMo_{11}W$) was prepared by acidifying the sodium salt, $Na_2HPMo_{11}WO_{40}$[19] was prepared from an appropriate mixture solution of 85% H_3PO_4 (5.8 mL), $Na_2MoO_4 \cdot 2H_2O$ (99% purity) (152.8 g), $Na_2WO_4 \cdot 2H_2O$ (99% purity) (18.9 g) and $HClO_4$ (70%) in 400 mL of distilled water. The mixture was then acidified by 40 mL of 37% HCl, and the acidic $H_3PMo_{11}WO_{40}$ was extracted by 400 mL Et_2O.

The heteropolysalt $K_3PMo_{11}WO_{40}$ (noted as $KPMo_{11}W$) was prepared by a precipitation method.[20] 10 g of $HPMo_{11}W$ was dissolved in 50 mL distilled water and then, this solution was added to a saturated KCl (99.5% purity) (5M) solution (20 mL distilled water containing 30 g KCl) with vigorous stirring for 20 min. The precipitate $K_3PMo_{11}WO_{40}$ appeared quickly which was washed and dried under vacuum.

The heteropolycompound $K_{2.5}Fe_{0.08}H_{0.26}PMo_{11}WO_{40}$ (noted as $KFePMo_{11}W$) was prepared according to the literature.[3,21] An aqueous solution (0.08 mol.L^{-1}) of $Fe(NO_3)_3$ (99.99% purity) was added dropwise to an aqueous solution of $HPMo_{11}W$ (0.06 mol.L^{-1})) at 50 °C, followed by the addition of an aqueous solution (0.08 mol.L^{-1}) of KCl (99.5% purity) under vigorous stirring, resulting in immediate precipitation of $KFePMo_{11}W$ salt. Stirring continued until complete evaporation of the solvent at room temperature. The powder was collected without washing, and ground in the mortar.

2.2 *Characterization*

The specific surface area S_{BET}, average pore diameter d_p and pore volume V_{pN2} of all the heteropolycompounds were determined by N_2 adsorption-desorption method at liquid N_2 temperature using a Quantachrome apparatus. Prior to the measurements, the samples were degassed at 150 °C and 10^{-5} Pa. The BET specific surface area was calculated by using the standard Brunauer, Emmett and Teller method on the basis of the adsorption data. The pore size distributions were calculated applying the Barrett-Joyner-Halenda (BJH) method to the desorption branches of the isotherms. FTIR spectra of the heteropolycompounds were obtained on KBr pellets in the 400–4000 cm^{-1} wavenumber range using a Bio-Rad FTS 165 spectrometer. The XRD powder diagrams were obtained on a Siemens "D5000" diffractometer with Cu Kα radiation. The diffractograms were recorded in (5–60°) 2θ range. Solid-state ^{31}P MAS NMR spectra were obtained on a Bruker Avance II 500 spectrometer operating at 202.5 MHz. The chemical shifts were referenced to $Al(PO_3)_3$. The UV measurements of the catalysts (dissolved in acetonitrile/water 1:1 ratio, the aqueous solutions had a concentration of 10^{-5} M) were made using a UV-VIS spectrophotometer Shimadzu UV-2100 PC at λ = 190–400 nm in 1 cm quartz cuvettes.

Acid-base properties of heteropolycompounds (HPC) were determined by an indirect method consisting of the test of isopropanol (IPA) decomposition. This reaction was tested in a continuous-flow fixed-bed reactor between 100 and 200 °C, atmospheric pressure, feed 5 wt% IPA in nitrogen, with a flow 40 $cm^3 \cdot min^{-1}$. The reaction products (propylene, di-isopropyether and acetone) were quantified by gas chromatography (Shimadzu 14B) with a flame ionisation detector (FID). A Carbowax 20M on a Chromosorb W column was used for separation of the products.

2.3 *Catalytic tests*

Catalytic activity tests were made in a stainless steel tubular fixed bed reactor (6 mm diameter and 400 mm length) at atmospheric pressure in the temperature range 300–400 °C. A sample of 200 mg of catalyst was pre-treated in an oxygen stream at a flow rate of 2 L/h for 1 h at the reaction temperature. The reactant gaseous mixture was obtained by bubbling CO_2 or N_2O at a flow rate of 2 L/h into liquid in saturator with ethylbenzene (vapor pressure of 4.13 kPa) at 53 °C. CO_2 or N_2O was added to the flow in a molar ration of 10:1 to ethylbenzene. After the reaction, the flowing gas containing eventually ethylbenzene, styrene, acetophenone, α-methyl benzyl alcohol, benzene, ethene and CO_x was analyzed online by a Shimadzu GC-14 B gas chromatograph equipped with two detectors (TCD/FID,) and with two columns filled with 5 Å molecular sieve and SE-30 10% CW respectively. The experimental data were recorded after 8 h of reaction. Schematic diagram of the experimental setup used for oxidative dehydrogenation ethylbenzene (Figure S1 in Supplementary Information).

Ethylbenzene (EB) conversion and Styrene (STY) selectivity have been calculated as following equations:

$$\text{EB Conversion}(\%) = \frac{\text{moles of EB}_{in} - \text{moles of EB}_{out}}{\text{moles of EB}_{in}} \times 100$$

$$\text{STY Selectivity}(\%) = \frac{\text{moles of STY}_{out}}{\text{moles of all products}_{out}} \times 100$$

3. Results and Discussion

3.1 *Characterization of the catalysts*

3.1a *Textural properties of heteropolycompounds:*: The BET surface area of the solids determined from N_2 adsorption–desorption isotherms are shown in Table 1. The total or partially substituted salts presented high surface area compared to the pure acid as already reported by several authors.[22,23] The $KFePMo_{11}W$ salts displayed lower surface area (190 m^2/g) than the potassium salts $KPMo_{11}W$ (220 m^2/g) and the proton containing heteropolyacid $HPMo_{11}W$ showed lower surface area (5 m^2/g) than the heteropolysalts. It was found that introducing the iron in $KFePMo_{11}W$ structure, the

Table 1. Textural parameters of various heteropolycompounds.

Heteropolycompounds	Surface area (m^2/g)	Pore volume, V_{IP} (cm^3/g)	Pore diameter, d_m (nm)
$HPMo_{12}$	3	0.010	12
$HPMo_{11}W$	5	0.012	14
$KPMo_{11}W$	220	0.202	25
$KFePMo_{11}W$	191	0.178	19

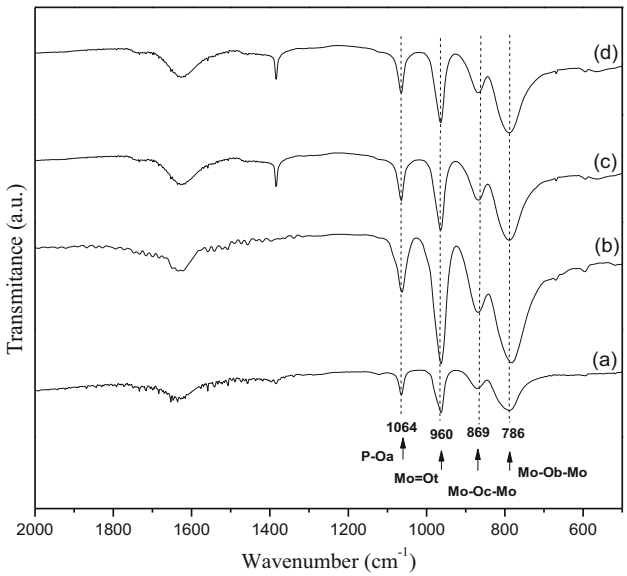

Figure 1. IR spectra: (a) $HPMo_{12}$, (b) $HPMo_{11}W$, (c) $KPMo_{11}W$, and (d) $KFePMo_{11}W$.

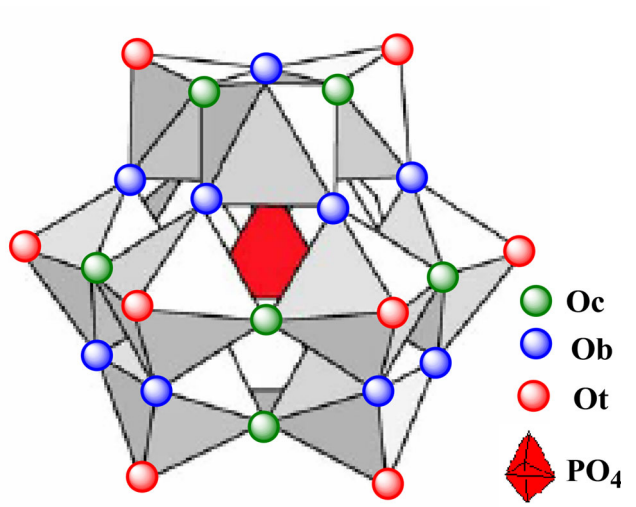

Figure 2. The schematic structure of Keggin anion $(PMo_{12}O_{40})^{3-}$.

surface area significantly decreased (190 m^2/g). Diminishing of specific surface area could be explained owing to heteropolycompound pores blocked by iron, as well as by the formation of some HPAs crystallite agglomeration. The pore diameter and pore volume of the sample is increased more than the pure acids (14 to 25 nm and 0.012 to 0.202 cm^3/g).

3.1b *Fourier-transform infrared spectroscopy*: Infrared spectra of $HPMo_{12}$, $HPMo_{11}W$, $KPMo_{11}W$ and $KFePMo_{11}W$ are given in Figure 1. All the spectra are very similar with tiny variations in the positions of absorption bands. They present the characteristic features of the Keggin anion with bands at 1065, 960, 870 and 785 cm^{-1}, which were assigned to P-O_a (O_a = oxygen belonging to the central PO_4 tetrahedron), Mo=O_t (O_t= terminal oxygen), interoctahedral Mo-O_b-Mo (O_b = bridged oxygen of two octahedral sharing a corner), and intraoctahedral Mo-O_c-Mo (O_c = bridged oxygen sharing an edge) vibrations, respectively.[18] The schematic structure of Keggin anion $(PMo_{12}O_{40})^{3-}$ is shown in Figure 2.

3.1c *UV-Visible spectra*: The electronic absorption spectra of heteropolyanions wwere observed in the range of 200–500 nm. The intense electronic spectra in the UV–Vis region exhibited by the Keggin-structure polyoxometallates have been experimentally assigned as O → M ligand-to-metal charge transfer. Bulk $HPMo_{12}$ shows the absorption bands at 216 and 310 nm, while $HPMo_{11}W$ at 216 and 270 nm (Figure 3), they are assigned to the O_t → M (O_t: terminal oxygen) and O_b/O_c → M (O_b or O_c: bridge-oxygen) charge-transfer transition.[24,25] The UV spectra of $KPMo_{11}W$ and $KFePMo_{11}W$ are very similar to the spectrum of heteropolyacid $HPMo_{11}W$.

3.1d *X-ray diffraction studies*: The XRD pattern of the acidic $HPMo_{12}$ and $HPMo_{11}W$ are presented in Figure 4. There were peaks in four groups in the ranges of 2θ: 5–10°, 17–22°, 25–30°, and 31–37°, in agreement with the characteristic peaks of the Keggin structure. The diffractograms of $HPMo_{12}$and $HPMo_{11}W$ agree with the existence of a single crystallographic phase with a pattern typical of a triclinic system.[24] $KPMo_{11}W$ and $KFePMo_{11}W$ (Figure 4), exhibit three strong diffraction peaks at 2θ = 10.6°, 26.4° and 36.0°, which are characteristic of the cubic phases and all major reflections can be indexed, using a Rietveld profile analysis, on the basis of a cubic unit cell (space group Pn3m) with

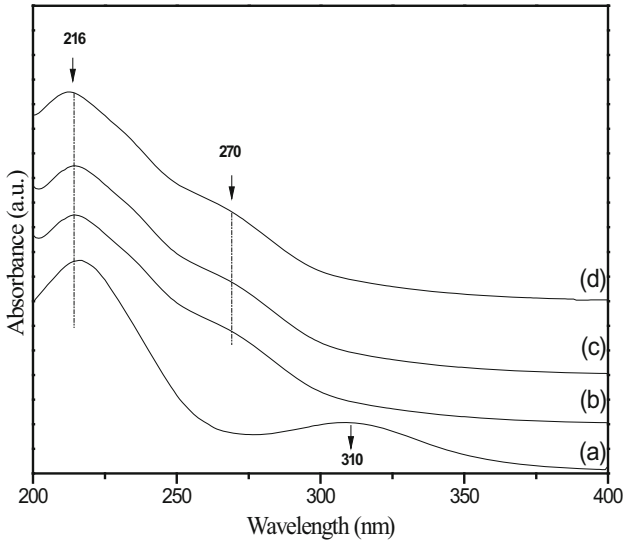

Figure 3. UV–VIS spectra: (a) $HPMo_{12}$, (b) $HPMo_{11}W$, (c) $KPMo_{11}W$, and (d) $KFePMo_{11}W$.

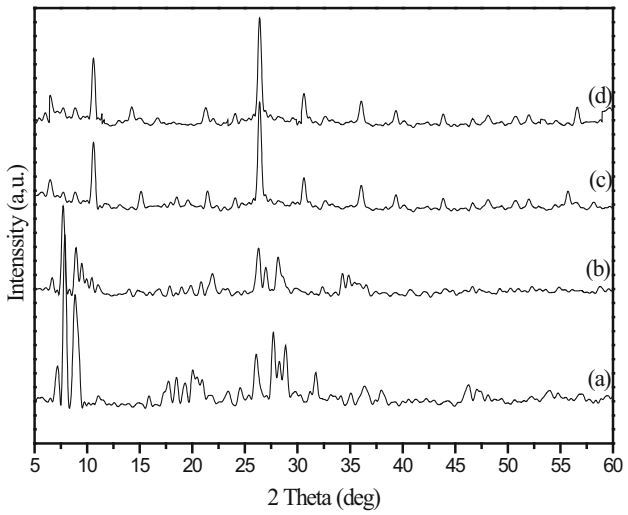

Figure 4. XRD patterns: (a) $HPMo_{12}$, (b) $HPMo_{11}W$, (c) $KPMo_{11}W$, and (d) $KFePMo_{11}W$.

a = 11.6920 Å.[26] It is important to note that two diffraction peaks at 2θ = 15.1° and 21.4° only appear for the catalysts containing K.

3.1e *Solid-state ^{31}P NMR*: Solid-state ^{31}P MAS NMR of $HPMo_{12}$ (Figure 5) showed a single peak at -3.70 ppm. For the $PMo_{11}W$ compounds, the isotropic component consists of different narrow peaks distributed over *ca* 5 ppm, which corresponds to a distribution of mixed $PMo_{12-x}W_x$ anions.[27]

3.1f *Isopropanol decomposition*: Isopropanol decomposition has long been considered as a chemical probe reaction for surface acid-base properties.[28,29] Isopropanol undergoes dehydration to give propylene

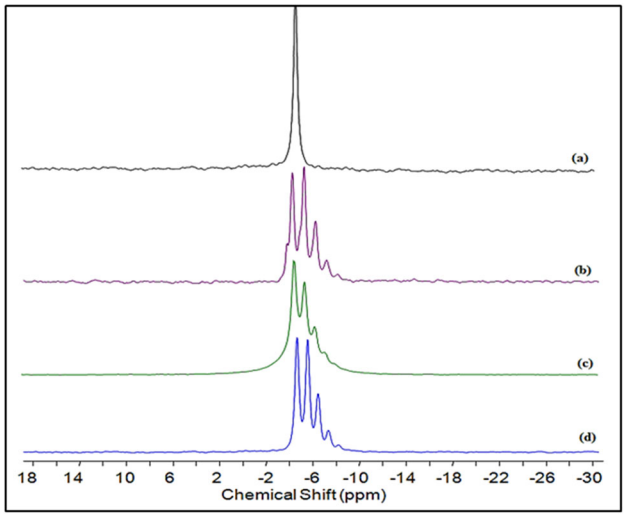

Figure 5. ^{31}P MAS NMR spectra of: (a) $HPMo_{12}$, (b) $HPMo_{11}W$, (c) $KPMo_{11}W$, and (d) $KFePMo_{11}W$.

on acidic surface sites and dehydrogenation *via* a concerted mechanism on adjacent acidic and basic surface sites to give acetone.

The results obtained from the isopropanol decomposition using heteropolycompounds as catalysts as a function of reaction temperature are presented in Table 2. It is clear that $HPMo_{11}W$ and $KFePMo_{11}W$ are the most active catalysts. The high activity can be correlated with increasing the surface acidity associated with the presence of protons in Keggin structure. Propene is the major reaction product. However, it is also observed that when the protons in the parent acids are partially exchanged by iron and potassium cations ($KFePMo_{11}W$) they enhance the stationary state activity of the parent acids Table 2. This can be attributed to the partial hydrolysis of the polyanion during preparation, which formed weakly acidic H^+. On the contrary, when the substitution of the proton of $HPMo_{11}W$ by K ion ($KPMo_{11}W$) occurs, the initial activity decreased, resulting in relatively lower conversion than the $HPMo_{11}W$ and $KFePMo_{11}W$. This decrease is attributed to the decrease in the number and the strength of the acid sites of the catalyst. The presence of redox species Mo^{6+}/Mo^{5+}, W^{6+}/W^{5+} and Fe^{3+}/Fe^{2+} in the catalysts can contribute to dehydration and dehydrogenation in the decomposition of isopropanol.

3.2 *Catalytic behavior*

Ethylbenzene oxidation was studied at different temperatures from 300 to 400 °C on the various polyoxometalates as catalysts using CO_2 and N_2O as the oxidant. In the dehydrogenation of ethylbenzene in the presence

Table 2. Results on the catalytic activity of POMs at different temperatures in isopropanol decomposition.

Catalyst	T (°C)	Conversion (%)	Products Selectivity (%)		
			Propylene	Di-isopropylether	Acetone
$HPMo_{12}$	100	17	60	30	10
	150	60	80	13	07
	200	90	92	04	04
$HPMo_{11}W$	100	20	58	36	06
	150	70	82	06	12
	200	99	88	04	08
$KPMo_{11}W$	100	05	82	12	06
	150	32	90	09	01
	200	45	98	02	-
$KFePMo_{11}W$	100	20	80	05	15
	150	80	62	03	35
	200	98	70	-	30

Table 3. The effect of N_2O and CO_2 on catalytic proprieties.

Catalyst	T (°C)	(%) Ethylbenzene Conversion		(%) Styrene Selectivity		(%) Benzene Selectivity		(%) Ethene Selectivity		(%) Oxygenates Selectivity	
		N_2O	CO_2	N_2O	CO_2	N_2O	CO_2	N_2O	CO_2	N_2O	CO_2
$HPMo_{12}$	300	07	05	45	66	36	25	19	09	-	-
	350	10	07	61	75	28	19	11	06	-	-
	400	13	09	70	80	25	17	05	03	-	-
$HPMo_{11}W$	300	15	17	72	31	15	40	13	29	-	-
	350	23	18	83	66	11	15	06	19	-	-
	400	25	20	92	90	04	06	04	04	-	-
$KPMo_{11}W$	300	03	04	100	100	-	-	-	-	-	-
	350	07	06	100	100	-	-	-	-	-	-
	400	04	04	100	100	-	-	-	-	-	-
$KFePMo_{11}W$	300	18	06	93	100	05	-	02	-	-	-
	350	40	32	35	60	10	31	07	09	48	-
	400	46	34	30	48	22	29	11	13	37	-

Oxygenates: α-methyl benzyl alcohol, acetophenone and benzoic acid

of N_2O, the reaction products are mainly styrene, benzene, α-methyl benzyl alcohol, acetophenone, ethene and carbon oxide. Using CO_2 as an oxidizing agent in this reaction, only styrene, benzene and carbon monoxide were obtained. Table 3 summarizes the experimental results for the conversion of ethylbenzene as well as the styrene selectivity in the oxidative dehydrogenation of ethylbenzene in the presence of CO_2 and N_2O.

Over $HPMo_{12}$, at two reactions temperatures, ethylbenzene conversion does not exceed 10% using CO_2 or N_2O as the oxidant and the highest selectivity to styrene obtained with CO_2 as oxidant was about 75% at 350 °C. When one atom of molybdenum is replaced by tungsten in Keggin structure, $HPMo_{11}W$ improves the ethylbenzene conversion significantly. At any temperature, ethylbenzene conversion is higher over $HPMo_{11}W$ than that over $HPMo_{12}$, while the styrene selectivities are similar to those observed over $HPMo_{12}$. Substitution of tungsten as an addendum atom produces a more favorable strong acidic sites for catalyzing dealkylation and oxidation reactions. At 300 °C, over $HPMo_{12}$, using CO_2 or N_2O, ethylbenzene conversion does not exceed 7% and the best selectivity to styrene (66%) was observed in the CO_2 atmosphere. At the same temperature, over $HPMo_{11}W$, ethylbenzene conversion reached 17% with CO_2 and 15% using N_2O but the highest selectivity to styrene was obtained with N_2O (72%). This behaviour may be assigned to the increase of the Brønsted acid when replacing Mo^{6+} by W^{6+} in the Keggin anion.[24] The low selectivity in styrene observed at 300 °C on both catalysts is attributed to the high surface acidity of catalyst that promotes dealkylation reaction at the expense of dehydrogenation reaction. Upon increasing the reaction temperature, the styrene selectivity increased, which

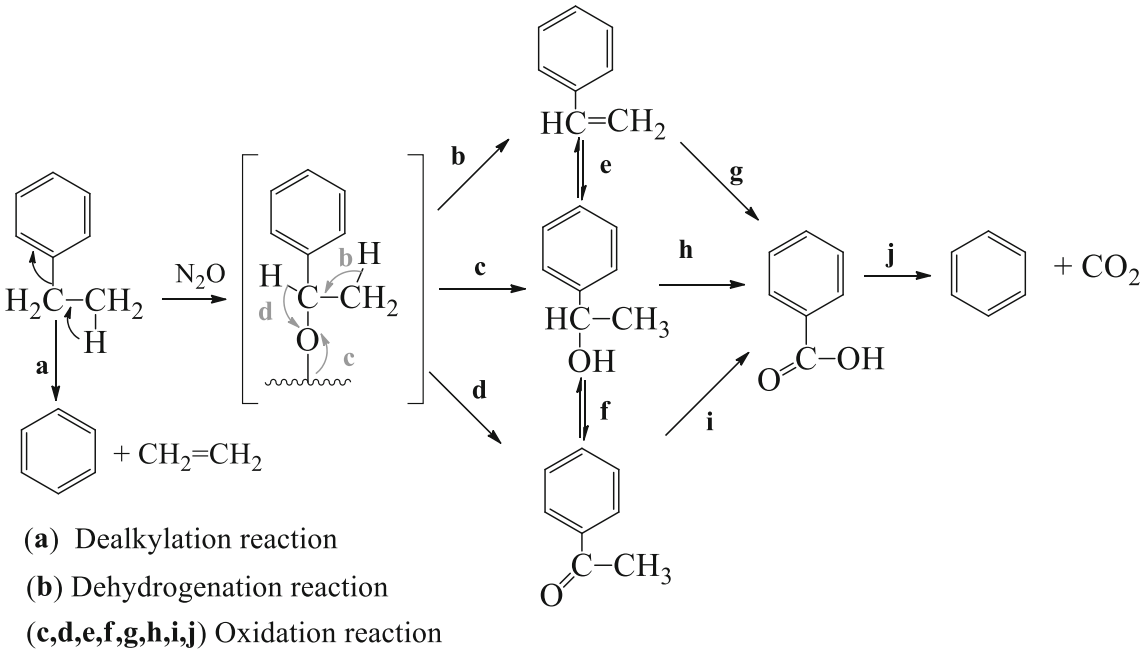

Figure 6. Reaction pathways for the oxidative dehydrogenation of ethylbenzene by N_2O.

could be explained by a decrease in Brönsted acidity on the catalyst surface. At a reaction temperature of 400 °C, over $HPMo_{11}W$, styrene selectivity using CO_2 or N_2O reached 90% and 92%, respectively, while the ethylbenzene conversion was slightly higher than those observed at 350 °C. At this temperature, the sample is decomposed in mixed oxides such as P_2O_5, MoO_3 and WO_3. This increase in styrene selectivity may be favoured by the decrease of the acidic sites of the catalysts, thus suppressing the dealkylation reactions compared to the dehydrogenation reaction. Both oxidation and dealkylation reactions take place simultaneously on the surface of the catalyst leading to styrene and benzene. The formation of benzene and ethene is a result of dealkylation reaction predominating on acid sites, whereas on redox sites Mo^{6+}/Mo^{5+}, oxidative dehydrogenation of ethylbenzene takes place leading to styrene or to α-methyl benzyl alcohol, acetophenone, benzoic acid and carbon dioxide. This suggests that both oxidative dehydrogenation and simple dehydrogenation reaction are probably present in the catalyst when N_2O is used as the oxidant, as shown in Figure 6.

Over $KPMo_{11}W$ salt, in the presence of CO_2, the catalytic activity is similar to that under N_2O, independent of reaction temperature. Over this catalyst, ethylbenzene conversion was decreased dramatically compared to those results obtained with corresponding acid ($HPMo_{11}W$). At all temperatures, ethylbenzene conversion did not exceed 7% with N_2O and 6% using CO_2. With $KPMo_{11}W$ catalyst, at all reactions temperatures, it was found that incorporating alkaline metals

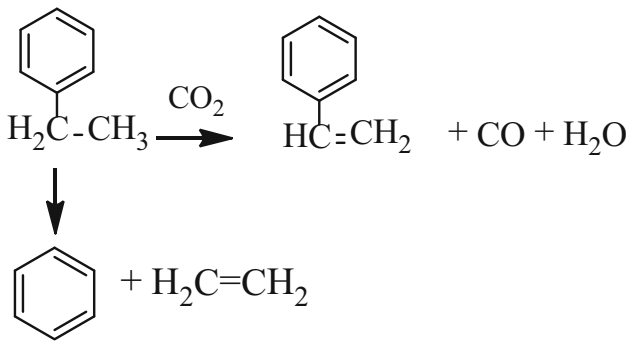

Figure 7. Reaction pathways for the oxidative dehydrogenation of ethylbenzene by CO_2.

decreased the conversion of ethylbenzene but increases the selectivity to styrene (100%). These results suggest that the absence of acid sites favours the oxidative dehydrogenation reactions.[24] Over $KFePMo_{11}W$ catalyst, ethylbenzene conversion increases with increasing reaction temperature, while the selectivity to styrene showed an opposite response to temperature. The decrease in the styrene selectivity could be attributed to two factors: an increase in the oxidation of styrene to the oxygenate products and dealkylation of ethylbenzene to benzene. Under similar reaction conditions, ethylbenzene conversion was higher with N_2O as oxidant than with CO_2. A higher selectivity to styrene was obtained with CO_2 than with N_2O as oxidant at all reaction temperature and all conversion. Carbon dioxide can react with ethylbenzene to give styrene, benzene, CO and H_2O. The reaction seems to proceed as shown in Figure 7.

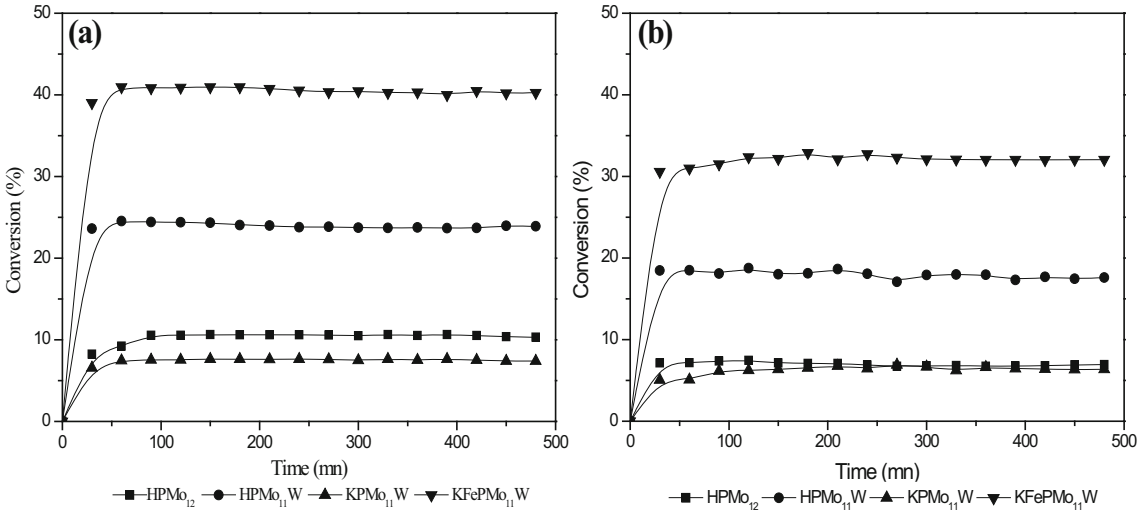

Figure 8. Time-on-stream at 350 °C on ethylbenzene conversion with (a) N_2O and (b) CO_2.

At 350 °C, over $KFePMo_{11}W$, 40% conversion can be obtained using N_2O but the selectivity to styrene was dropped (35%), while the selectivity to the oxygenates was increased (48%). This result indicated that the initial product, styrene was further oxidized to α-methyl benzyl alcohol, acetophenone and benzoic acid when N_2O is used as the oxidant. Under similar reaction conditions, ethylbenzene conversion did not exceed 10%, 23% and 7% with N_2O and 7%, 18% and 6% with CO_2 over $HPMo_{12}$, $HPMo_{11}W$ and $KPMo_{11}W$, respectively. The $KFePMo_{11}W$ was found to be active catalyst for the ethylbenzene conversion in the presence of nitrous oxide or carbon dioxide. However, the reaction selectivity depended strongly on the chemical environment and redox proprieties of iron (Fe). Reaction temperature of 300 °C appeared to be more selective in the styrene formation (100% with CO_2 and 93% with N_2O); the presence of iron outside Keggin structure alters the acid-base properties of the catalyst, which in turn influences the catalytic behaviour. Whereas, at 350 °C, $KFePMo_{11}W$ showed a higher selectivity of oxygenates products (48%) such as α-methyl benzyl alcohol, acetophenone and benzoic acid. This suggests that iron in this cationic site increases the acidity and accelerates more the redox process. This has been explained by the presence of Fe_2O_3 or Fe_3O_4 species which could increase the Lewis acidity and redox proprieties. Among the factors determining the catalytic properties of iron HPA-based catalysts, the redox behavior of iron is known to play a key role in oxidative dehydrogenation and oxidation of hydrocarbons in accordance with Mars-van-Krevelen mechanism.[30] Consequently, it can be proposed that facile redox cycle between fully oxidized and reduced iron species yields a catalyst which is more effective.

The variation of ethylbenzene conversion was studied as a function of the reaction time. Figure 8a shows that the catalytic activity is initially low, then it increases in about 1 h to a steady-state for all heteropolycompounds using nitrous oxide as the oxidizing agent. The steady-state conversion of 40% was readily obtained for $KFePMo_{11}W$. Whereas, with carbon dioxide (Figure 8b), the steady-state was reached only after several hours (more than 3 h). The conversion increases from an initial low value to the steady-state value of 30% for the same catalyst. These results revealed that the presence of K-Fe as counter-ions display an improved effect on the activity and stability of the catalyst in the oxidative dehydrogenation of ethylbenzene reaction.

4. Conclusions

Heteropolycompound catalysts were observed to react at a relatively low temperature (300–400 °C) compared to oxide catalysts, which work at 550–650 °C. Coupling the N_2O decomposition with the ethylbenzene dehydrogenation seems to be a very effective and selective process for styrene production. The novel catalyst $KFePMo_{11}W$ exhibited high catalytic performance as solid acids particularly for reactions in the gas phase. The use of CO_2 gas as oxidant for the oxidative dehydrogenation (ODH) ethylbenzene results in the formation of styrene as the highly selective product.

Supplementary Information (SI)

Experimental set up and Spectra (Figures S1–S9) and Tables S1–S3 are available as Supplementary Information at www.ias.ac.in/chemsci.

References

1. Dimitratos N and Védrine J C 2003 Role of acid and redox properties on propane oxidative dehydrogenation over polyoxometalates *Appl. Catal*. **81** 561
2. Nowinska K, Wacław A, Sopa M and Klak M 2002 Heteropoly compounds as precursors of catalysts for oxydehydrogenation of ethane *Catal. Lett*. **78** 347
3. Mizuno N, Tateishi M and Iwamoto M Pronounced Catalytic Activity of $Fe_{0.08}Cs_{2.5}H_{1.26}PMo_{11}VO_{40}$ for Direct Oxidation of Propane into Acrylic Acid 1995 *Appl*. *Catal. A: Gen*. **128** 165
4. Langpape M, Millet J-M M, Ozkan U S and Delichère P 1999 Study of Cesium or Cesium Transition Metal-Substituted Keggin-Type Phosphomolybdic Acid as Isobutane Oxidation Catalysts: II. Redox and Catalytic Properties *J. Catal*. **182** 148
5. Min J-S and Mizuno N 2001 Effects of additives on catalytic performance of heteropoly compounds for selective oxidation of light alkanes *Catal. Today* **71** 89
6. Shilov A E and Shulpin G B 1997 Activation of C-H Bonds by Metal Complexes *Chem. Rev.* **97** 2879
7. Liu S, Chen L, Wang G, Liu J, Gao Y, Li C and Shan H 2016 Effects of Cs-substitution and partial reduction on catalytic performance of Keggin-type phosphomolybdic polyoxometalates for selective oxidation of isobutene *J. Energy Chem*. **25** 85
8. Ma B, Zhang Z, Song W, Xue X, Yu Y, Zhao Z and Ding Y 2013 Solvent-free selective oxidation of C H bonds of toluene and substituted toluene to aldehydes by vanadium-substituted polyoxometalate catalyst *J. Mol. Catal. A: Chem.* **368** 152
9. Zhang J, Sun M, Cao C, Zhang Q, Wang Y and Wan H 2010 Effects of acidity and microstructure on the catalytic behavior of cesium salts of 12-tungstophosphoric acid for oxidative dehydrogenation of propane *Appl. Catal. A: Gen.* **380** 87
10. Sri Hari Kumar A, Upendar K, Qiao A, Rao P S N, Lingaiah N, Kalevaru V N, Martin A, Sailu C and Sai Prasad P S 2013 Selective oxidative dehydrogenation of ethane over MoO_3/V_2O_5–Al_2O_3 catalysts: Heteropolymolybdate as a precursor for MoO_3 *Catal. Commun.* **33** 76
11. Woodle G B 2005 Ethylbenzene In *Encyclopedia of Chemical Processing* Vol. 1 Sunggyu Lee (Ed.) (New York, USA: CRC Press)
12. Cavani F and Trifiro F 1995 Alternative processes for the production of styrene *Appl. Catal. A Gen.* **133** 219
13. Oganowski W, Hanuza J, Drulis H, Migta W and Macalik L 1996 Promotional effect of molybdenum, chromium and cobalt on a V-Mg-O catalyst in oxidative dehydrogenation of ethylbenzene to styrene *Appl. Catal. A: Gen.* **136** 143
14. Zhang Z, Zhao Z and Xu C 2005 Research advances in the catalysts for the selective oxidation of ethane to aldehydes *Chin. Sci. Bull*. **50** 833
15. Bulánek R and Novoveská K 2003 Oxidative dehydrogenation of propane by nitrous oxide and/or oxygen over Co beta zeolite *React. Kinet. Catal. Lett*. **80** 337
16. Nakagawa K, Okumura K, Shimamura T, Ikenaga N, Suzuki T, Kobayashi T, Nishitani-Gamo M and Ando T 2003 Novel selective oxidation of light alkanes using carbon dioxide, Oxidized diamond as a novel catalytic medium *Chem. Lett.* **32** 866
17. Ramudu P, Anand N, Mohan V, Murali D G, Sai Pasad P S, David R B and Seetha R R K 2015 Studies on ethylbenzene dehydrogenation with CO_2 as soft oxidant over Co_3O_4/COK-12 catalysts *J. Chem. Sci.* **127** 701
18. Rocchiccioli-Deltcheff C, Fournier M, Franck R and Thouvenot R 1983 Vibrational investigations of polyoxometalates. 2. Evidence for anion-anion interactions in molybdenum (VI) and tungsten (VI) compounds related to the Keggin structure *Inorg. Chem*. **22** 207
19. Misono M, Mizuno N, Katamura K, Kasai A, Konishi Y, Sakata K and Yoneda Y 1982 Catalysis by Heteropoly Compounds. III. The Structure and Properties of 12-Heteropolyacids of Molybdenum and Tungsten ($H_3PMo_{12-x}W_xO_{40}$) and Their Salts Pertinent to Heterogeneous Catalysis *B. Chem. Soc. Jpn.* **55** 400
20. Jing F, Katryniok B, Bordes-Richard E and Paul S 2013 Improvement of the catalytic performance of supported $(NH_4)_3HPMo_{11}VO_{40}$ catalysts in isobutane selective oxidation *Catal. Today* **203** 32
21. Mizuno N, Tateishi M and Iwamoto M 1994 Enhancement of Catalytic Activity of $Cs_{2.5}Ni_{0.08}H_{0.34}PMo_{12}O_{40}$ by V^{5+} Substitution for Oxidation of Isobutane into Methacrylic Acid *Appl. Catal. A Gen*. **118** 1
22. Essayem N, Coudurier G, Fournier M and Védrine J 1995 Acidic and catalytic properties of $Cs_xH_{3-x}PW_{l2}O_{40}$ heteropolyacid compounds *Catal. Lett*. **34** 223
23. Gayraud P Y, Stewart I H, Derouane-Abd Hamid S B, Essayem N, Derouane E G and Védrine J C 2000 Performance of potassium 12-tungstophosphoric salts as catalysts for isobutane/butene alkylation in subcritical and supercritical phases *Catal. Today* **63** 223
24. Okuhara T 1996 Catalytic Chemistry of Heteropoly Compounds *Adv. Catal.* **41** 113
25. Youn M H, Kim H, Jung J C, Song I K, Barteau K P. Barteau M A 2005 UV–vis spectroscopy studies of $H_3PMo_{12-x}W_xO_{40}$ heteropolyacid (HPA) catalysts in the solid state: Effects of water content and polyatom substitution *J. Mol. Catal. A: Chem.* **241** 227
26. Goubin F, Guénée L, Deniard P, Koo H J, Whangbo M H, Montardi Y and Jobic S 2004 Synthesis, optical proprieties and electronic structures of polyoxometalates $K_3PMo_{12-x}W_x$ *J. Solid State Chem*. **177** 4528
27. Tadaharu U, Takashi T and Masashi H 2004 ^{31}P NMR and Raman spectroscopic and voltammetric studies on the formation and conversion processes of Keggin-type molybdotungstophosphate(V) and arsenate(V) complexes in aqueous-organic solvents *Inorg. Chim. Acta* **357** 59
28. Gervasini, A Fenyvesi J and Auroux A 1997 Study ofthe acidic character ofmodified metal oxide surfaces using the test of isopropanol decomposition *Catal. Lett*. **43** 219
29. Ai M and Suzuki S 1973 Oxidation Activity and Acidity of MoO_3-P_2O_5Catalysts *J. Catal*. **30** 362
30. Mars P and van Krevelen D W 1954 Oxidations carried out by means of vanadium oxide catalysts *Chem. Eng. Sci.* **3** 41